Antibodies for the Treatment of Bone Diseases: Preclinical Data

9

Wolfgang Sipos

9.1 Animal Models of Osteoporosis

9.1.1 General Aspects

Osteoporosis is a complex systemic disease (Pietschmann et al. 2008). Therefore, researchers have to rely on rodent and large animal models for the development of new antiosteoporotic therapeutics. Rodent models are well established and have been widely used in osteoporosis research. However, the US Food and Drug Administration (FDA), besides rats, also demands the use of large animal models in preclinical testing of antiosteoporotic substances with an experimental time frame of 12 months when using rats and 16 months when using larger species. According to FDA regulations, valid animal models have to develop an osteoporotic phenotype either spontaneously or after ovariectomy (OVX) (FDA Guidelines 1994). In order to give an idea of the different biomechanical forces on the skeletons of small vs large animal species, Fig. 9.1 shows the skeletons of a rat, a sheep, and a minipig. There exist several ways of inducing osteopenia or osteoporotic phenotypes in mammals, such as *OPG* gene knockout, systemic RANKL administration, prolonged glucocorticoid administration, age-related osteoporosis, dietary calcium shortage, OVX, and combinations. All these manipulations have specific advantages and disadvantages, and the physiological relevance has to be proven for each model. Although calcium shortage itself may induce osteopenia to some extent, it is usually combined with OVX, which may be considered the main model of postmenopausal and thus estrogen deficiency-induced osteoporosis.

In this context it is essential to be aware of species-specific sexual endocrinology. Whereas women (and macaques) have a sexual cycle of 28 days, sows experience spontaneous ovulations as well but with a cycle length of 21 days. With regard

W. Sipos, DVM
Clinical Department for Farm Animals, University of Veterinary Medicine Vienna, Vienna 1210, Austria
e-mail: Wolfgang.Sipos@vetmeduni.ac.at

P. Pietschmann (ed.), *Principles of Osteoimmunology*,
DOI 10.1007/978-3-319-34238-2_9

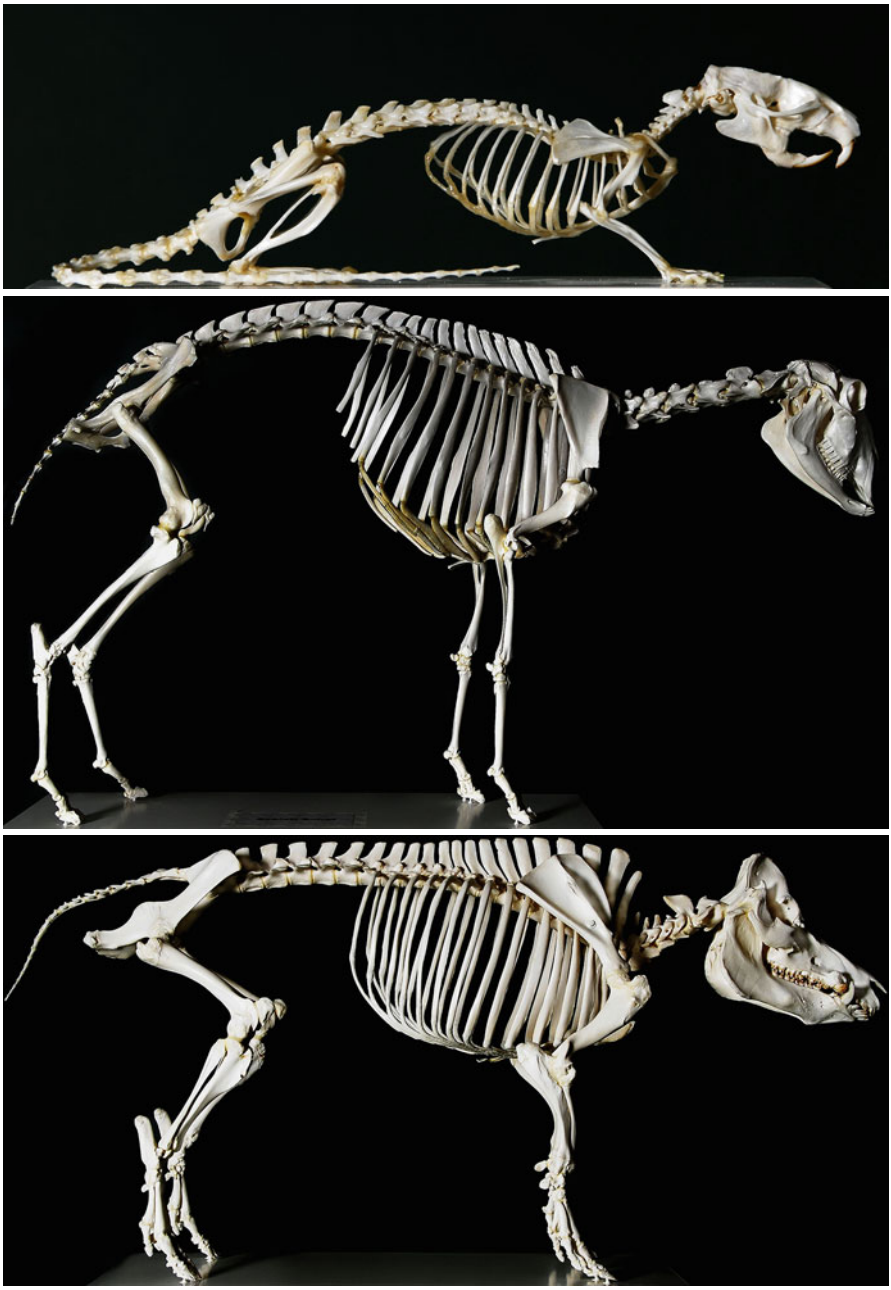

Fig. 9.1 Skeletons of a rat, a sheep, and a minipig. Not only due to large differences concerning body weight but also due to the different position of extremities in relation to the body and different functions of the vertebral column with regard to ensuring the stability of thorax and especially the abdomen between the shown species, interspecies differences concerning the mechanical forces exerting an impact on the axial and the appendicular skeletons are the logical consequence (Photos with kind permission of G. Weissengruber, Vienna)

to sheep, there are seasonal and aseasonal breeds with a mean cycle length of 17 days. The seasonal rhythm is regulated by the epiphyseal melatonin secretion, which is significantly higher in winter ("short day breeders"). The mainly used merinos are an aseasonal breed. Another feature, which has to be kept in mind, is extragonadal estrogen synthesis, which may cause a rebound effect in ovariectomized sheep in terms of lowering bone mineral density (BMD) change differences when compared to sham animals starting from 4 months after OVX (Sigrist et al. 2007). Moreover, ovariectomized sows experience extragonadal estrogen synthesis to some extent (Sipos et al. 2011a). Female dogs are seasonal monestric, usually in March and September. Heat includes proestrus, estrus, and early metestrus and takes 3 weeks. Estradiol increases only during this very short period to titers between 18 and 50 pg/ml during proestrus and decreases already after the start of estrus to baseline levels of 5 pg/ml (Sipos 1997). Rats have sexual cycles of 4–5 days, whereas mice experience inducible ovulations. Furthermore, the occurrence of a natural menopause has not been proven in all model animals, except for macaques.

Nevertheless, estrogen deficiency induced by OVX leads to an osteoporotic phenotype in rodents as well as diverse ungulates and can be aggravated by additional glucocorticoid administration or calcium shortage. However, it has to be kept in mind that osteoporosis as defined for humans (i.e., osteopenia plus fragility fractures due to disturbed cortical and trabecular microarchitecture) does not naturally occur in our domestic mammals. Therefore, all models have their weaknesses. In this chapter, we will focus on rodent and artiodactyl models, but largely spare canine as well as primate models, as these are used less frequently due to ethical reasons, although especially primate models most closely reflect the situation in humans.

9.1.2 Rodent Models

In contrast to large animal models, there is a broad range of genetically modified rodent models. *OPG*$^{-/-}$ mice suffer from severe osteoporosis associated with a high incidence of fractures and vertebral deformities but lack unwanted side effects on immune function, which can be observed in *RANKL*$^{-/-}$ mice (Bucay et al. 1998; Kong et al. 1999; Yun et al. 2001). Systemic RANKL administration also leads to increased osteoclast numbers and to an osteoporotic phenotype in mice (Lacey et al. 1998). Prolonged glucocorticoid exposure by subcutaneously implanted slow-release prednisolone pellets (2.1 mg/kg/day) is another reasonable means of inducing osteoporosis in rodents (Weinstein et al. 1998). Wang et al. (2001) demonstrated an age-related decline of bone mass in the axial and appendicular skeleton and a decrease in bone formation in the spine in aged male Sprague–Dawley rats. Pietschmann et al. (2007) described similar changes, i.e., markedly reduced cancellous bone mineral density (BMD), bone volume (BV), and trabecular number (Tb.N), in the proximal tibiae of aged male rats. Additionally, bone formation as well as osteoclastogenesis appeared decreased, which was substantiated by decreased insulin-like growth factor 1 (IGF-1), osteocalcin, and RANKL serum levels. Bone density and bone strength are reduced in young growing rats by dietary

calcium restriction in the range of 0.3–2.5 g Ca^{2+}/kg diet (Thomas et al. 1988; Persson et al. 1993; Talbott et al. 1998).

In the rat, rapid loss of cancellous bone mass and strength occurs following OVX, which after a while reaches a steady-state phase of bone mass with an increase in the rate of bone turnover (Wronski et al. 1986, 1988, 1989, 1990; Wronski and Yen 1992; Kalu 1991). The proximal tibial metaphysis, the lumbar vertebral bodies, and the femoral neck are affected by cancellous bone loss within 1 month after OVX, whereas OVX-induced bone loss does not occur in the trabecular bone of long bone epiphyses, the distal tibial metaphysis, and the caudal vertebrae (Ma et al. 1994; Li et al. 1996; Westerlind et al. 1997; Miyakoshi et al. 1999). The situation of the cortical bone in the ovariectomized rat is complex, as increased bone resorption taking place at the endosteum of the diaphysis of long bones is antagonized by stimulated periosteal bone growth (Turner et al. 1987; Miller et al. 1991; Aerssens et al. 1996). Thus, enlargement of the marrow cavity is the most sensitive index of cortical bone loss in this species. As the rat, like most other experimental animal models, does not experience naturally occurring pathological fractures, bone strength has to be tested mechanically. Significant loss of vertebral and femoral neck bone strength occurs 3 months after OVX (Mosekilde et al. 1991; Mosekilde et al. 1993a; Peng et al. 1994; Sogaard et al. 1994; Jiang et al. 1997; Yoshitake et al. 1999). Reduction of dietary calcium from 0.4 to 0.2 % in ovariectomized rats results in a further decrease in bone density and mechanical properties (Shahnazari et al. 2009).

Alternative rodent osteoporosis models include the Botox-induced and the LPS-induced bone loss models (Grimston et al. 2007; Ochi et al. 2010). In the former, mice are injected intramuscularly with 2.0 U Botox per 100 g body weight in the quadriceps, hamstrings, and posterior calf muscles of one hind limb. Maximum limb dysfunction occurs by days 2–3 after Botox injection without gender differences. By 3–4 weeks postinjection, full activity is restored. Bone loss in the injected limb is rapid and profound with the difference to the noninjected limb being significant by week 2. At 12 weeks trabecular BV in the injected limb is substantially reduced, and cortical thickness is lowered. In the endotoxin model, male adult mice are subcutaneously injected with 20 mg/kg LPS. LPS treatment reduces BV/TV for approximately 40 % in the proximal region of tibial bones by 48 h posttreatment. This LPS-induced enhancement of osteoclastogenesis can be blocked by OPG administration giving evidence of the importance of RANKL signaling in this setting, but LPS or OPG does not affect osteoclastogenesis in *TNFR1*$^{-/-}$ mice. Interestingly, osteoblast surface is remarkably reduced in these mice as a result of enhanced osteoblast apoptosis due to TRAIL-mediated signaling, which triggers apoptosis of primary osteoblasts only when the TNFR1 signal is ablated in vitro.

9.1.3 Ovine Models

There is also a bulk of literature dealing with the ovine species and its suitability as a postmenopausal osteoporosis model. The compact bone of growing sheep is predominantly plexiform. A well-developed Haversian system consisting of secondary

osteons is not developed until an age of 7–9 years (Turner 2002; Pearce et al. 2007). Seasonal fluctuations in bone metabolism complicate the interpretation of data. It should also be mentioned that biochemical bone metabolism markers are regarded as having only limited informative value in the ovine model (Gerlach 2002). Due to anatomical peculiarities of ovine vertebrae, biomechanical parameters fail to correlate with BMD of these bone sites, but do so with femoral BMD. Anatomical features of the iliac crest seem to be close to the corresponding human bone site (Ito et al. 1998). Although sheep do not experience a natural menopause, decreasing bone mass in aging sheep might prove this species a potential model for age-related osteoporosis (Turner et al. 1993). OVX alone is not as efficient as in other species, whereas glucocorticoid treatment induces an osteoporotic phenotype comparable to the one in other species including humans (Chavassieux et al. 1993; Hornby et al. 1995). BMD of L5 and distal radius as evaluated by DXA is significantly changed 6 months and the one of L4 1 year after OVX, whereas the proximal parts of the femur, humerus, and tibia do not exhibit changes to that extent (Turner et al. 1995). However, MacLeay et al. (2004) were not able to detect areal BMD changes in lumbar vertebrae in ovariectomized sheep 3 months after surgery. Another study showed a significantly decreased femoral but not lumbar vertebral BMD as well as significant effects on cortical bone parameters by 6 months after OVX (Chavassieux et al. 2001). Interesting and seemingly inconsistent with the likelihood of extragonadal estrogen synthesis is the fact that sheep experience significant microarchitectural changes in the vertebral cancellous bone (decreased BV/TV by approximately 30 %, trabecular thickness (Tb.Th) by 13 %, and increased trabecular separation (Tb.Sp) by 46 %) 2 years after OVX and show histomorphometric changes (i.e., significantly increased osteoclast numbers) already 3 months after surgery (Giavaresi et al. 2001; Pogoda et al. 2006).

Combining OVX with profound dietary calcium restriction (1.5 g Ca^{2+} and 100 IU $VitD_3$/day instead of the physiological daily need for 4–5 g Ca^{2+} and 1.000 IU $VitD_3$/day) and weekly doses of 120–200 mg methylprednisolone in 7–9 years old ewes for 7 months led to an approximately 35–40 % reduction of BMD of the spongiosa of the radius and tibia without affecting the corticalis (Lill et al. 2002). Lumbar vertebral bodies exhibited a decrease in BMD of 13 %. Also, all analyzed histomorphological parameters of the iliac crest as well as BV/TV of L4, and Tb.Th, BV/TV, and bone surface (BS/BV) of femoral head were significantly altered and corresponded well with biomechanical data. Although the profound decrease of BMD of approximately 4 SD is remarkable in this model, the increased susceptibility for opportunistic infections and the drawbacks concerning osteoimmunological analyses due to the prolonged exposure to glucocorticoids have to be considered. Another study showed the advantages of combining OVX and glucocorticoid administration over combining OVX and calcium restriction with a higher decrease of BMD of the distal radius, distal tibia, and calcaneus (the spongiosa by 25 % and the corticalis by 17 % in the former group and 10 and 5 % in the latter, respectively) (Lill et al. 2000). Combining all three measures led to the most pronounced reductions (60 and 25 %). Age dependency of osteoporosis inducibility in sheep is still a matter of debate, but there is some consensus that inducing measures should last at least 7 months, and the time span between OVX and lactation should be over a year due to the increased

intestinal calcium resorption (Hornby et al. 1995; Lill et al. 2002). Chavassieux et al. (1993) induced osteoporosis in adult ewes by daily intramuscular (IM) injections of 30 mg methylprednisolone for 2 months followed by 15 mg for 1 month. Mineral apposition rate in the iliac crest was decreased by 63 %, and bone formation rate was decreased by 84 %.

9.1.4 Porcine Models

Pigs seem to have some advantages over sheep concerning their suitability as biomedical large model species because of several anatomical and physiological reasons. Although there are a lot of similarities of diverse porcine organ systems to their human orthologs, the pig's usefulness as an osteological model species is still not entirely clear. However, the porcine femoral compact bone is predominantly plexiform, but is converted to well-developed osteonal bone earlier than in sheep (Mori et al. 2005). Peak bone mass is obtained with an age of 2–3 years. Ovariectomized and calcium-restricted (0.3 % Ca^{2+}) multiparous conventional sows seem not to be ideal models for osteoporosis research, most probably due to their extremely high mean areal BMD of 1.5 g/cm^2 as measured at the femoral neck, which seemingly reduces bone plasticity (Sipos et al. 2011a). Contrary, growing pigs aged 2 months have a mean areal BMD of 0.64 g/cm^2 as measured by DXA (Sipos et al. 2011b). Therefore, the main body of investigations in this area of research was performed using growing minipigs, which, however, might not appropriately reflect the situation of the postmenopausal osteoporotic woman due to their juvenile age. On the other hand, minipigs achieve sexual maturity earlier than conventional pigs, and thus OVX may induce the desired phenotype earlier than in conventional sows. Mosekilde et al. (1993b) successfully established a minipig bone loss model. OVX in 10-month-old minipigs resulted in a 6 % decrease in BMD, 15 % in BV, and 13 % in Tb.N, and an increase of 15 % in Tb.Sp after 6 months, whereas OVX in combination with a mild nutritive calcium shortage (0.75 % Ca^{2+}), which had already been started at an age of 4 months, led to a 10 % reduction in vertebral BMD and significant increases in final erosion depth and vertebral marrow star volume. In the growing pig model, calcium restriction (0.1–0.4 %) for 1 month leads to increased plasma PTH, calcitriol, alkaline phosphatase (ALP), propeptide of type 1 procollagen (P1CP), and hydroxyproline titers, which are associated with osteoporotic changes of metacarpals (Eklou-Kalonji et al. 1999). A study investigating multiparous sows being fed a standard diet (1.5 Ca^{2+}) showed a significant increase in plasma PTH, calcitriol, and AP levels over a time span of 1 year after OVX (Scholz-Ahrens et al. 1996). This could not be reproduced by our group in a similar setting (Sipos et al. 2011a). However, the former group also did not observe significant bone morphometric changes.

Whereas glucocorticoid treatment alone has been shown not to be sufficient to induce osteoporosis in the ovine model, this does not apply to the porcine model (Scholz-Ahrens et al. 2007). In adult (30 months old) primiparous Göttingen minipigs, an osteoporotic phenotype could be induced by daily oral treatment with 1 mg/

kg of prednisolone for 2 months and a reduction to 0.5 mg/kg thereafter until the end of the experiment, which was after 8 months in the short-term group and 15 months in the long-term group. In the short term, glucocorticoids reduced BMD at the lumbar spine by 48 mg/cm^3 from baseline, whereas in the control group the reduction was 12 mg/cm^3. These changes were also evidenced by plasma BAP levels, which decreased significantly in the glucocorticoid group. In the long term, the loss of BMD became more pronounced and bone mineral content, Tb.Th, and mechanical stability tended to be lower compared to the control group. There was a negative association between the cumulative dose of glucocorticoids and BMD, which could be traced back to impaired osteoblastogenesis. Other authors used growing minipigs (Ikeda et al. 2003). They treated 8-month-old Göttingen minipigs subcutaneously with prednisolone at a dosage of 0.5 mg/kg, 5 days/week for 26 weeks. Glucocorticoid treatment significantly reduced bone turnover marker (serum osteocalcin, urinary type-1 collagen N-telopeptide) levels at 13 weeks and thereafter also serum BAP levels relative to baseline. At 26 weeks, the longitudinal axis of the lumbar vertebral bone and length of the femur were smaller in the glucocorticoid group compared to the control group. The same applied to the BMD of the femur, but not L2, as measured by DXA. Age-dependent increases in trabecular bone structure were also reduced by glucocorticoids. L2 and femora of these animals were also tested mechanically, and prednisolone was shown to significantly reduce the ultimate load and maximum absorption energy of both sites. Further regression analyses revealed that bone minerals, bone structure, and chemical markers correlated with mechanical properties of L2 and mid-femur. It was concluded that prednisolone reduced systemic bone formation and resorption and suppressed the age-dependent increases in bone minerals, structure, and mechanical properties of L2 and mid-femur.

9.2 Animal Models of Rheumatoid Arthritis

Like osteoporosis, rheumatoid arthritis (RA) is a very complex pathological condition. Whereas this has not been proven for osteoporosis, rheumatoid arthritis is clearly identified as an autoimmune disease with a chronic inflammatory character. Although the responsible autoantigens are still speculative (most seemingly cyclic citrullinated peptides), there are several models, which reflect the pathophysiological situation satisfactorily on the focal (including redness, joint swelling, cartilage, and bone destruction) as well as the systemic level with upregulated proinflammatory cytokines. In the following, the most frequently used models will be presented in short: adjuvant-induced arthritis (AIA), collagen-induced arthritis (CIA), and the TNF-α transgenic mouse. Contrary to biomedical osteoporosis research, in rheumatoid arthritis research only rodent models are used.

Classically, AIA is induced by an intradermal injection of heat-killed *Mycobacterium tuberculosis* in paraffin oil at the base of the tail followed by a consecutive injection into one knee joint. The clinical onset is 9 days following the second injection as indicated by hind paw swelling and locomotory difficulties

(Feige et al. 2000). In a modified protocol, mice are immunized intradermally at the base of the tail and four footpads with 100 mg of methylated BSA (mBSA) emulsified in an equal volume of complete Freund's adjuvant (Ohshima et al. 1998). Additionally, mice are intraperitoneally injected with *Bordetella pertussis*. This procedure is repeated 7 days later. On day 21, 100 mg of mBSA in 10 ml of saline is injected into one knee joint. As a control, the same volume of saline is injected into the contralateral one. The acute phase of AIA lasts for 1 week starting after the booster injection and is followed by a chronic phase. Mice usually are sacrificed 35 days after the first immunization.

CIA is elicited by an intradermal injection or intravenous infusion of heterologous type II collagen emulsified 1:1 with incomplete Freund's adjuvant (Cremer et al. 1983; Stolina et al. 2009a). Following other regimens, CIA is induced after intradermal immunization with collagen emulsified in complete Freund's adjuvant, followed by a booster dose of collagen emulsified in incomplete Freund's adjuvant 3 weeks later. Disease susceptibility is strongly linked to the MHC class II haplotype. CIA-susceptible mice such as DBA/1, B10.Q, and B10.III are the most commonly used strains for the CIA model. Mice should be young (approx. 8 weeks) and healthy, and in many settings male mice are preferred because they develop disease earlier than females. CIA is consistently induced 16–35 days after immunization in 90–100 % of male mice and in 60–100 % of females using bovine collagen. Notably, progression of the two models, AIA and CIA, is mediated by distinct immunopathogenic mechanisms (Cremer et al. 1983). With respect to the dominant pro-arthritic cytokines, AIA is driven mainly by TNF-α (Stolina et al. 2009b), while CIA is provoked mainly by IL-1 (Stolina et al. 2008). Of importance for a systemic proinflammatory disease is that both CIA and AIA are characterized by a systemic upregulation of acute-phase proteins, IL-1β, IL-8, CCL2, and RANKL, whereas TNF-α, IL-17, and PGE_2 are elevated exclusively in clinical AIA. In contrast, Sarkar et al. (2009) found in their CIA model that joint inflammation was associated with a higher ratio of systemic IL-17/IFN-γ. Interestingly, neutralization of IFN-γ accelerated the course of CIA and was associated with increased IL-17 levels in serum and joints. The authors concluded that the absolute level of IL-17 is not the only determinant of joint inflammation. Instead, the balance of Th1, Th2, and Th17 cytokines is suggested to control the immune events leading to joint inflammation.

More recently, the serum transfer arthritis model has been generated. This model is based on T cells expressing a single autoreactive TCR recognizing glucose-6-phosphate isomerase (G6PI). These cells escape negative selection in mice bearing a specific MHC class II allele, IAg7. In the periphery, these T cells promote a breach in B cell tolerance, and high levels of anti-G6PI antibodies are produced, leading to a destructive and erosive arthritis similar to that seen in human RA. The adoptive transfer of serum from these mice results in peripheral joint swelling in most recipient strains. Early events that trigger paw swelling in the serum transfer model include signaling through FcRs. Further analysis demonstrated that $Fc\gamma RII^{-/-}$ mice manifested accelerated arthritis whereas $Fc\gamma RIII^{-/-}$ mice experienced a more slowly progressing arthritis. In the K/BxN serum transfer model of arthritis, there is a clinically apparent acute phase, which is modulated by FcγRII and FcγRIII, and a

subacute component, which results in bone erosion, even in the absence of FcγR signaling (Corr and Crain 2002).

The TNF-α transgenic mouse (Keffer et al. 1991) allows deregulated human *TNF-α* gene expression. These mice develop a chronic inflammatory and destructive polyarthritis within 6 weeks after birth (Redlich et al. 2002).

9.3 Animal Models of Cancer-Associated Osteolytic Lesions

Many aggressively growing malign entities metastasize into the bone causing osteolytic lesions, which relies on the RANKL-mediated osteoclastogenesis-promoting nature of these tumor cells. Among the clinically most relevant bone-affecting tumors are the sexual steroid-controlled mammary and prostate cancers as well as multiple myeloma. In rodent mammary cancer models, usually the human breast cancer cell line MDA-231 is injected into the left ventricle of female athymic BALB/c nude mice aged 4–8 weeks under general anesthesia (Mbalaviele et al. 1996; Morony et al. 2001). Transplanted mice develop a profound cachexia. Multiple osteolytic lesions with highly active osteoclasts are evident in the bones of the proximal and distal extremities within 1 month after tumor inoculation.

More sophisticated data than those produced by radiography can be acquired by means of in vivo whole-body bioluminescence imaging (BLI). This technique demands the application of luciferase (*Luc*)-gene transduced cells of interest. Visibility is induced by a preceding intraperitoneal injection of luciferin (Canon et al. 2008). For example, BLI has been applied in the 4 T1 model. The 4 T1 orthotopic breast cancer model has been extensively utilized to examine the efficacy of a series of bisphosphonate compounds for the treatment of breast cancer bone metastases (Yoneda et al. 2000). This model is characterized by the occurrence of bone metastases in nearly 100 % of animals. Histological examination reveals the occurrence of profound osteoclastic bone resorption, and luciferase activity assays confirm tumor burden (Reinholz et al. 2010). In the 4 T1/Luc model, washed 4 T1 luc-transduced mouse mammary cancer cells are suspended in sterile PBS and subcutaneously injected into mammary fat pads of 4–5-week-old syngeneic female BALB/c mice. Primary mammary tumors form approximately 1 week after cell inoculation, and metastases to the lung and liver develop within 2 weeks. Metastases to the bone, adrenals, kidneys, spleen, and heart occur by 3 weeks post-inoculation. Mice typically succumb by 4 weeks after tumor cell injection.

Prostate cancer (PC) bone metastases can also be induced by intracardial tumor cell infusions into male nude mice (Miller et al. 2008). *Luc*-transduced cells were found to develop a pattern of bioluminescence consistent with tumor metastatic foci in the bone with the highest concentrations in hind limbs and mandible as early as 3–5 days after intracardial injection. Another route for administration of PC cells is the intratibial injection (Ignatoski et al. 2008). Herein, the hind limb is shaved, the knee cap is located, and cells are injected in a volume of 50 µl into the tibia percutaneously via the tibial crest into the marrow cavity.

Xenograft models are also utilized for inducing multiple myeloma-associated bone metastases. The KAS-6/1-MIP-1α mouse model may serve as an example (Reinholz et al. 2010). Herein, genetically engineered KAS-6/1 myeloma cells carrying the osteoclast activating factor MIP-1α are injected into female SCID mice. Bone loss occurs within 2 weeks, hind limb paralysis occurs within 2 months, and mice typically die 1 week later.

Other tumor cell types used for generating osteolytic bone metastases include human A431 epidermoid carcinoma cells and murine colon adenocarcinoma-26 cells. A431/Luc cells were found to cause osteolytic lesions in the hind limbs after 20 days, and Colon-26 cells colonize the skeleton and cause significant localized bone destruction in syngeneic 7–8-week-old BALB/c DBA/2 mice within 12 days after intracardial tumor inoculation (Morony et al. 2001; Canon et al. 2010).

9.4 Immunotherapy of Osteoporosis in Animal Models

9.4.1 Osteoprotegerin as Surrogate for Denosumab in Rodent Models

The following two subchapters focus on RANKL blockade in rodent and non-primate large animal models. First, the effects of RANKL blockade have been investigated in models of postmenopausal osteoporosis. Fewer preclinical data are available for this treatment option of male osteoporosis. Min et al. (2000) demonstrated the protective and osteoporosis-reversing effects of the treatment of *OPG*$^{-/-}$ 8-week-old mice with high intravenous doses of 50 mg/kg of recombinant human (rh) OPG three times per week for 4 weeks. The advantage of rhOPG, which is fused to an Fc fragment, is its sustained serum half-life enabling a prolonged antiresorptive activity. In a next step, Capparelli et al. (2003) treated male, 10-week-old Sprague–Dawley rats with a single intravenous bolus injection of 5 mg/kg rhOPG. Maximum rhOPG concentrations were seen within 12 h after injection and coincided with significant elevations of serum PTH levels, which normalized 24 h later. Although a remarkable decline in rhOPG serum levels started at day 10, rhOPG serum concentrations remained at measurable levels throughout the 30-day study. The suppression of osteoclastic bone resorption started within 24 h after treatment. Significant gains in tibial cancellous BV were evident within 5 days. Femoral BMD increased between days 10 and 20. The significant decrease of osteoclast surface of 95 % in the rhOPG group was paralleled by a 35 % decrease in the serum bone resorption marker TRAP5b. Repeated rhOPG treatment (5 times 2 mg/kg within 2 weeks) further led to an increase of bone fracture strength at the femur mid-diaphysis in three-point bending by 30 % without affecting elastic or maximum strength in young male Sprague–Dawley rats (Ross et al. 2001). At the femoral neck, rhOPG significantly increased elastic (45 %), maximum (15 %), and fracture (35 %) strengths. Additionally, rhOPG treatment significantly increased whole bone dry mass (25 %), mineral mass (30 %), organic mass (17 %), and percent mineralization (4 %). Overall, rhOPG augments mineralization

and strength indices in the rat femur with its effects on strength being more pronounced in the femoral neck than at the mid-diaphysis.

Next, effects of RANKL blockade have been tested in diverse osteoporosis models. Ominsky et al. (2008) treated ovariectomized rats aged 3 months with 10 mg/kg rhOPG twice weekly. OVX was associated with significantly higher serum RANKL titers, increased osteoclast surface, and reduced areal and volumetric BMD. Recombinant human OPG markedly reduced osteoclast surface and serum TRAP5b while completely preventing OVX-associated bone loss in the lumbar vertebrae, distal femur, and femoral neck. μCT analyses showed that trabecular compartments in rhOPG-treated OVX rats had a significantly greater BV fraction, volumetric BMD, bone area, Tb.Th, and Tb.N. Additionally, rhOPG improved the cortical area in the lumbar vertebrae and femoral neck to levels that were significantly greater than in OVX or sham controls. Also, bone strength was increased in OVX rats by rhOPG treatment.

Clinical development of rhOPG was discontinued in favor of denosumab. Thus, preclinical experiments demanded a rodent model in which this fully humanized monoclonal antibody that specifically inhibits primate and human RANKL would be effective. Preliminary experiments showed that denosumab did not suppress bone resorption in normal mice or rats but prevented the resorptive response in mice challenged with a human RANKL fragment encoded primarily by the fifth exon of the RANKL gene. Therefore, exon 5 from murine RANKL was replaced by its human ortholog. The resulting huRANKL mice exclusively express chimeric (human/murine) RANKL that maintains bone resorption at slightly reduced levels when compared to wild-type controls (Kostenuik et al. 2009). In these mice denosumab reduced bone resorption, increased cortical and cancellous bone mass, and improved trabecular microarchitecture. Hofbauer et al. (2009) analyzed the bone protective effects of denosumab (10 mg/kg subcutaneously twice weekly over 4 weeks) in glucocorticoid-treated male, 8-month-old homozygous huRANKL knock-in mice. They showed that prednisolone treatment induced the loss of vertebral and femoral volumetric BMD, which was associated with suppressed vertebral bone formation and increased bone resorption as evidenced by increases in the number of osteoclasts, TRAP5b protein in bone extracts, serum levels of TRAP5b, and urinary excretion of deoxypyridinoline. More detailed analysis showed that glucocorticoid-induced bone loss was most pronounced in the cortical and subcortical compartment in the distal femoral metaphysis whereas trabecular BMD remained unchanged by prednisolone treatment. Denosumab prevented prednisolone-induced loss of total BMD at the spine and the distal femur. Additionally, biomechanical compression tests of lumbar vertebrae revealed a detrimental effect of prednisolone on bone strength that could also be prevented by denosumab.

In analogy to rhOPG and denosumab as RANKL antagonists, Kim et al. (2009) developed a cell-permeable inhibitor termed RANK receptor inhibitor (RRI), which targets a cytoplasmic motif of RANK. The RRI peptide blocked RANKL-induced osteoclast formation from murine bone marrow-derived macrophages. Furthermore, RRI inhibited the resorptive function of osteoclasts, induced osteoclast apoptosis,

and protected against OVX-induced bone loss in mice. As RANK blockade may theoretically impair the immune system, the authors also determined whether the RRI peptide interferes with phagocytosis or dendritic cell differentiation; both immune functions were not affected.

Li et al. (2009a) tested the effects of rhOPG treatment on bone biology of orchiectomized (ORX) rats. Whereas serum testosterone declined within 2 weeks after surgery, no changes in serum RANKL could be observed. In contrast, there was an increase of RANKL in bone marrow plasma, which correlated positively with marrow plasma TRAP5b. RANKL inhibition was induced by treating ORX rats twice weekly for 6 weeks subcutaneously with 10 mg/kg rhOPG. Whereas vehicle-treated ORX rats showed significant deficits in BMD of the femur and tibia as well as lower trabecular BV in the distal femur, rhOPG treatment increased femoral and tibial BMD and trabecular BV to levels that significantly exceeded values for ORX or sham controls. Histologically, rhOPG treatment reduced trabecular osteoclast surfaces in ORX rats by 99 %. µCT of lumbar vertebrae from rhOPG-treated ORX rats demonstrated significantly greater cortical and trabecular bone volume and density versus ORX-vehicle controls. These data substantiate RANKL inhibition as a strategy for preventing bone loss associated with androgen ablation or deficiency.

9.4.2 Osteoprotegerin as Surrogate for Denosumab in Pigs

Data on the effects of rhOPG treatment in large animal models are limited. The homology between a porcine RANKL-specific sequence and the corresponding human RANKL sequence was found to be 79 %. Also, RANKL is upregulated during in vitro osteoclastogenesis and expressed by a variety of different cell types including immunocytes in pigs (Sipos et al. 2005). Sipos et al. (2011b) analyzed the effects of a single intravenous rhOPG bolus of 5 mg/kg in pigs aged 2 months. Serum rhOPG levels peaked at day 5 and coincided with significantly decreased calcium, phosphate, and bone turnover markers. TRACP5b, P1CP, and BAP levels significantly decreased by 40–70 % relative to vehicle controls in the rhOPG group between days 5 and 10, indicating that pharmacologic concentration of rhOPG led to systemic concomitant inhibition of bone formation and resorption. At termination of the experiment at day 20, µCT analysis showed a significantly higher connectivity density in the proximal femur, proximal tibia, and L4 as well as BMD of the femur, hip, and tibia. Interestingly, Tb.Th (femur, hip, L4) was significantly lower in the rhOPG-treated pigs, but Tb.N (femur) was higher, and a trend toward lower Tb.Sp was evident in the tibia. In summary, rhOPG treatment inhibited osteoclast function as evidenced by TRAP5b decrease and led to a more arborescent architecture and higher mineralisation in the weight-bearing skeleton. These data show that not only anatomical but also microstructural bone parameters as well as the responsiveness to RANKL inhibition may differ in detail between large mammal species such as humans and pigs and also between these species and rodents with their distinct biomechanical forces on the axial as well as the appendicular skeleton.

9.4.3 Romosozumab

Romosozumab is a humanized monoclonal antibody that targets sclerostin for the treatment of osteoporosis. Sclerostin is a potent inhibitor of the canonical Wnt signaling pathway, which is essential for osteoblastogenesis. Mutations in the sclerostin-encoding gene SOST lead to sclerostosis, which is the result of progressively increasing bone formation. Thus, romosozumab acts by supporting osteoblastogenesis, which is different from the final outcome achieved by denosumab, which exerts its effects by suppressing osteoclastogenesis.

In preclinical studies, the therapeutic potential of a neutralizing sclerostin antibody was tested in ovariectomized rats (Li et al. 2009b). This therapeutic intervention not only resulted in complete prevention of osteoporosis but had also strong osteoanabolic effects. In gonad-intact female cynomolgus macaques, the administration of a humanized neutralizing anti-sclerostin monoclonal antibody over 2 months had clear osteoanabolic effects with marked dose-dependent increases in bone formation on trabecular, periosteal, endocortical, and intracortical surfaces. Significant increases in trabecular thickness and bone strength were found at the lumbar vertebrae in the highest-dose group (Ominsky et al. 2010).

9.4.4 Secukinumab

Secukinumab is a human monoclonal antibody targeting IL-17A and is approved for the treatment of psoriasis. The therapeutic spectrum may soon be expanded to the treatment of uveitis, rheumatoid arthritis, ankylosing spondylitis, and psoriatic arthritis. Basis for the therapeutic application is the disturbance of the Th17/Treg balance in a large spectrum of diverse autoimmune diseases. Notably, also for osteoporosis the therapeutic use of anti-IL-17 antibodies has now been proposed, as a reduction of proinflammatory cytokines, an increase in regulatory T cell number, a positive effect on cortical as well as trabecular bone and bone mechanical parameters, and an increased osteoblastogenesis could be demonstrated in ovariectomized mice, which was even superior to anti-RANKL and anti-TNF-α antibodies (Tyagi et al. 2014). These effects may be considered as another hint toward an involvement of a dysregulation of the immune system in the pathogenesis of osteoporosis.

9.5 Immunotherapy of Rheumatoid Arthritis in Animal Models

Antirheumatic drugs exhibit pronounced adverse side effects. Therefore, efforts aim to establish more specific anti-inflammatory and osteoclastogenesis-inhibitory therapeutic regimens including RANKL blockade. First, rhOPG monotherapy was tested for its efficacy to ameliorate or abolish bone destructive processes of RA. In their study investigating male Lewis AIA rats treated with subcutaneously

administered rhOPG, Campagnuolo et al. (2002) found that rhOPG provided dose- and schedule-dependent preservation of BMD and periarticular bone while essentially eliminating intralesional osteoclasts. Dosages >2.5 mg/kg/day preserved or enhanced BMD and essentially prevented all erosions. OPG treatment was also successful in preventing the loss of cartilage matrix proteoglycans and was shown to be most effective when initiated early in the course of the disease. However, signs of inflammation could not be affected by rhOPG treatment. In another study based on TNF-α transgenic mice, the anti-inflammatory as well as anti-osteoclastogenic potential of infliximab, an anti-TNF-α monoclonal antibody, was compared to rhOPG and pamidronate treatment (Redlich et al. 2002). As may be delineated from the preceding study, clinical improvement was achieved only in the infliximab group. However, radiographic analyses revealed a significant retardation of joint damage in animals treated with rhOPG (55 % reduction of erosions), pamidronate (50 % reduction), a combination therapy of rhOPG and pamidronate (64 % reduction), and with infliximab (66 % reduction). These data show that rhOPG alone or in combination with bisphosphonates may be an effective therapeutic tool for the prevention of inflammatory bone destruction. Stolina et al. (2009a, b) also investigated Lewis rats with established AIA or CIA. Rats were treated with pegsunercept (a TNF-α inhibitor), anakinra (an IL-1 receptor antagonist), or rhOPG. Anti-TNF-α treatment ameliorated paw swelling in both models and reduced ankle BMD loss in AIA rats. Anti-IL-1 treatment decreased paw swelling in CIA rats and reduced ankle BMD loss in both models. Both anti-TNF-α and anti-IL-1 applications reduced systemic markers of inflammation as well as, at least in part, systemic RANKL, but failed to prevent vertebral BMD loss in either model. OPG reduced TRAP5b by over 90 % and consequently also BMD loss in ankles and vertebrae in both models, but as anticipated had no effect on paw swelling.

The former studies demonstrated that rat AIA and CIA feature bone loss and systemic increases in TNF-α, IL-1β, and RANKL. Anti-cytokine therapies targeting inflammatory cytokines consistently reduce inflammation in these models, but systemic bone loss often persists. On the other hand, RANKL inhibition consistently prevents bone loss without reducing joint inflammation. Logically, RANKL inhibition has to be further combined with anti-inflammatory, most preferably site-specific, drugs. Oelzner et al. (2010) treated AIA rats with dexamethasone (0.25 mg/kg/day, i.p.), rhOPG (2.5 mg/kg/day, i.p.), or a combination of both at regular intervals for 3 weeks. As expected, dexamethasone monotherapy substantially suppressed joint swelling without inhibiting bone loss of the secondary spongiosa, whereas rhOPG monotherapy showed no anti-inflammatory effect. Interestingly, rhOPG monotherapy failed to inhibit AIA-induced bone loss, whereas the combination of dexamethasone and rhOPG produced an anti-inflammatory effect and resulted in inhibition of periarticular and axial bone loss. Thus, the principle of combining an anti-inflammatory drug with RANKL inhibition may prove an effective bone-saving therapy in RA.

More recently, the disturbance of the Th17/Treg balance in the case of autoimmune diseases has come into focus of (pre)clinical research. Not only are these diseases characterized by a bias toward a Th17 activation, but it has also been

shown that these cells can even transdifferentiate out of regulatory T cells. The conversion of $Foxp3^{+}CD4^{+}$ T cells to Th17 cells was mediated by synovial fibroblast-derived IL-6 (Komatsu et al. 2014). The reestablishment of a preferable balance of Th17 cells to regulatory T cells can be achieved by different means, such as anti-IL17 antibodies or STAT3-inhibitors (Li et al. 2014; Park et al. 2014). Of notice, anti-IL17 treatment has the additional effect of indirectly suppressing also the expression of other proinflammatory cytokines, such as IL-1β and TNF-α (Li et al. 2014).

9.6 Immunotherapy of Cancer-Associated Osteolytic Lesions in Animal Models

RANKL is one of the key mediators of malignant bone resorption. Thus, RANKL inhibition prevents primary tumor or metastasis-induced osteolysis and decreases skeletal tumor burden. Morony et al. (2001) were among the first, who tested the ability of rhOPG to inhibit tumor-induced osteoclastogenesis, osteolysis, and skeletal tumor burden in two animal models. In one model they induced lytic bone lesions by transfecting mice with mouse colon adenocarcinoma (Colon-26) cells and found that treatment with rhOPG dose dependently decreased the number and area of radiographically evident lytic lesions with high efficacy. This therapeutic approach was also effective in nude mice transplanted with human MDA-231 breast cancer cells, completely preventing radiographic osteolytic lesions. Histologically, rhOPG decreased skeletal tumor burden by 75 % and completely eradicated MDA-231 tumor-associated osteoclasts. In both models, rhOPG had no effect on tumor metastases in soft tissue organs. The MDA-231 model for investigating the effects of RANKL inhibition in order to reduce bone tumor burden was also used by other authors, who confirmed the above findings. Investigating this model, Canon et al. (2008) found that RANKL protein levels were significantly higher in tumor-bearing bones than in tumor-free animals. They monitored the antitumor efficacy of RANKL inhibition by rhOPG on MDA-231 cells in a temporal manner using bioluminescence imaging. One mechanism by which RANKL inhibition reduced tumor burden appeared to be indirect through increasing tumor cell apoptosis as measured by active caspase-3. In this model, treatment with rhOPG resulted in an overall improvement in survival. Zheng et al. (2007) combined the antitumor effects of rhOPG and ibandronate, again using the MDA-231 mouse model. Ten days after intratibial tumor cell injection (when the tumors were evident radiologically), mice were treated with rhOPG (1 mg/kg/day), ibandronate (160 μg/kg/day), or a combination for 1 week, and the effects of each treatment on lytic lesions, tumor cell growth, cell apoptosis, and proliferation were measured. Compared to vehicle controls, treatment with all regimens prevented the expansion of osteolytic bone lesions at a similar rate (2.3 % increase in the mean vs 232.5 % increase in sham animals). Treatment with all regimens produced similar reductions in tumor area (mean 51.3 %) as well as a similar increase in cancer cell apoptosis (339.7 %) and decrease in cancer cell proliferation (59.7 %).

The inhibition of prostate cancer bone metastases is also subject of rodent model-based research. For treatment of metastatic hormone-refractory prostate cancer, docetaxel is a well-established medication. However, the side effects associated with docetaxel treatment can be severe, resulting in the discontinuation of therapy. Thus, efforts are ongoing to identify an adjuvant therapy to allow lower doses of docetaxel. As advanced prostate carcinomas are typically accompanied by skeletal metastases, targeting RANKL is a reasonable option. A combined treatment regimen based on RANKL inhibition and docetaxel decreased the establishment and progression of prostate carcinoma growth in the bone in murine models (Ignatoski et al. 2008). Fortunately, the combination of RANKL inhibition and docetaxel reduced tumor burden in the bone greater than either treatment alone and increased median survival time by 16.7 % (Miller et al. 2008).

Another study investigated whether the reduction of osteolysis by RANKL inhibition could enhance the antitumor effects of an anti-EGFR antibody (panitumumab) in a novel murine model of human A431 epidermoid carcinoma bone metastasis by bioluminescence imaging (Canon et al. 2010). As shown by earlier studies, these authors also found that RANKL inhibition by rhOPG treatment resulted in a reduction in tumor progression in bone sites and in tumor-induced osteolysis. The antitumor efficacy of panitumumab could be increased by rhOPG. The combination completely blocked tumor-induced bone breakdown. These studies demonstrate an additive effect of RANKL inhibition to the first-line agent in various murine bone metastasis settings and may lead to sanguine novel therapeutic options in the fight against tumor-associated bone diseases.

References

Aerssens J, van Audekercke R, Talalaj M, Geusens P, Bramm E, Dequeker J (1996) Effect of l-alpha-vitamin D3 and estrogen on cortical bone mechanical properties in the ovariectomized rat model. Endocrinology 137:1358–1364

Bucay N, Sarosi I, Dunstan CR, Morony S, Tarpley J, Capparelli C, Scully S, Tan HL, Xu WL, Lacey DL, Boyle WJ, Simonet WS (1998) Osteoprotegerin-deficient mice develop early onset osteoporosis and arterial calcification. Genes Dev 12:1260–1268

Campagnuolo G, Bolon B, Feige U (2002) Kinetics of bone protection by recombinant osteoprotegerin therapy in Lewis rats with adjuvant arthritis. Arthritis Rheum 46:1926–1936

Canon JR, Roudier M, Bryant R, Morony S, Stolina M, Kostenuik PJ, Dougall WC (2008) Inhibition of RANKL blocks skeletal tumor progression and improves survival in a mouse model of breast cancer bone metastasis. Clin Exp Metastasis 25:119–129

Canon J, Bryant R, Roudier M, Osgood T, Jones J, Miller R, Coxon A, Radinsky R, Dougall WC (2010) Inhibition of RANKL increases the anti-tumor effect of the EGFR inhibitor panitumumab in a murine model of bone metastasis. Bone 46:1613–1619

Capparelli C, Morony S, Warmington K, Adamu S, Lacey D, Dunstan CR, Stouch B, Martin S, Kostenuik PJ (2003) Sustained antiresorptive effects after a single treatment with human recombinant osteoprotegerin (OPG): a pharmacodynamic and pharmacokinetic analysis in rats. J Bone Miner Res 18:852–858

Chavassieux P, Pastoureau P, Chapuy C, Delmas PD, Meunier PJ (1993) Glucocorticoid-induced inhibition of osteoblastic bone formation in ewes: a biomechanical and histomorphometric study. Osteoporos Int 3:97–102

Chavassieux P, Garnero P, Duboeuf F, Vergnaud O, Brunner-Ferber F, Delmas PD, Meunier PJ (2001) Effects of a new selective estrogen receptor modulator (MDL 103,323) on cancellous and cortical bone in ovariectomized ewes: A biochemical, histomorphometric, and densitometric study. J Bone Miner Res 16:89–96

Corr M, Crain B (2002) The role of FcγR signaling in the K/BxN serum transfer model of arthritis. J Immunol 169:6604–6609

Cremer MA, Hernandez AD, Townes AS, Stuart JM, Kang AH (1983) Collagen-induced arthritis in rats: antigen-specific suppression of arthritis and immunity by intravenously injected native type II collagen. J Immunol 131:2995–3000

Eklou-Kalonji E, Zerath E, Colin C, Lacroix C, Holy X, Denis I, Pointillart A (1999) Calcium-regulating hormones, bone mineral content, breaking load and trabecular remodeling are altered in growing pigs fed calcium-deficient diets. J Nutr 129:188–193

FDA Guidelines (1994) Guidelines for Preclinical and Clinical Evaluation of Agents Used for the prevention or Treatment of Postmenopausal osteoporosis, Division of Metabolism and Endocrine Drug Products, Food and Drug Administration. Chapter: Preclinical Studies, 2–6

Feige U, Hu YL, Gasser J, Campagnuolo G, Munyakazi L, Bolon B (2000) Anti-interleukin-1 and anti-tumor necrosis factor-alpha synergistically inhibit adjuvant arthritis in Lewis rats. Cell Mol Life Sci 57:1457–1470

Gerlach UV (2002) Tierexperimentelles Modell zur Untersuchung der Frakturbehandlung beim osteoporotischen Knochen. Thesis, Justus-Liebig-Universität Giessen

Giavaresi G, Fini M, Torricelli P, Giardino R (2001) The ovariectomized ewe model in the evaluation of biomaterials for prosthetic devices in spinal fixation. Int J Artif Organs 24:814–820

Grimston SK, Silva MJ, Civitelli R (2007) Bone loss after temporarily induced muscle paralysis by Botox is not fully recovered after 12 weeks. Ann NY Acad Sci 1116:444–460

Hofbauer LC, Zeitz U, Schoppet M, Skalicky M, Schüler C, Stolina M, Kostenuik PJ, Erben RG (2009) Prevention of glucocorticoid-induced bone loss in mice by inhibition of RANKL. Arthritis Rheum 60:1427–1437

Hornby SB, Ford SL, Mase CA, Evans GP (1995) Skeletal changes in the ovariectomized ewe and subsequent response to treatment with 17β-estradiol. Bone 17:387–394

Ignatoski KM, Escara-Wilke JF, Dai JL, Lui A, Dougall W, Daignault S, Yao Z, Zhang J, Day ML, Sargent EE, Keller ET (2008) RANKL inhibition is an effective adjuvant for docetaxel in a prostate cancer bone metastases model. Prostate 68:820–829

Ikeda S, Morishita Y, Tsutsumi H, Ito M, Shiraishi A, Arita S, Akahoshi S, Narusawa K, Nakamura T (2003) Reductions in bone turnover, mineral, and structure associated with mechanical properties of lumbar vertebra and femur in glucocorticoid-treated growing minipigs. Bone 33:779–787

Ito M, Nakamura T, Matsumoto T, Tsurusaki K, Hayashi K (1998) Analysis of trabecular microarchitecture of human iliac bone using microcomputed tomography in patients with hip arthrosis with or without vertebral fracture. Bone 23:163–169

Jiang YB, Zhao J, Genant HK, Dequeker J, Geusens P (1997) Long-term changes in bone mineral and biomechanical properties of vertebrae and femur in aging, dietary calcium restricted and/or estrogen-deprived/-replaced rats. J Bone Miner Res 12:820–831

Kalu DN (1991) The ovariectomized rat as a model of postmenopausal osteopenia. Bone Miner 15:175–191

Keffer J, Probert L, Cazlaris H, Georgopoulos S, Kaslaris E, Kioussis D, Kollias G (1991) Transgenic mice expressing human tumour necrosis factor: a predictive genetic model of arthritis. EMBO J 10:4025–4031

Kim H, Choi HK, Shin JH, Kim KH, Huh JY, Lee SA, Ko CY, Kim HS, Shin HI, Lee HJ, Jeong D, Kim N, Choi Y, Lee SY (2009) Selective inhibition of RANK blocks osteoclast maturation and function and prevents bone loss in mice. J Clin Invest 119:813–825

Komatsu N, Okamoto K, Sawa S, Nakashima T, Oh-hora M, Kodama T, Tanaka S, Bluestone JA, Takayanagi H (2014) Pathogenic conversion of Foxp3+ T cells into TH17 cells in autoimmune arthritis. Nat Med 20:62–68

Kong YY, Yoshida H, Sarosi I, Tan HL, Timms E, Capparelli C, Morony S, Oliveira-dos-Santos AJ, Van G, Itie A, Khoo W, Wakeham A, Dunstan CR, Lacey DL, Mak TW, Boyle WJ, Penninger JM (1999) OPGL is a key regulator of osteoclastogenesis, lymphocyte development and lymph-node organogenesis. Nature 397:315–323

Kostenuik PJ, Nguyen HQ, McCabe J, Warmington KS, Kurahara C, Sun N, Chen C, Li L, Cattley RC, Van G, Scully S, Elliott R, Grisanti M, Morony S, Tan HL, Asuncion F, Li X, Ominsky MS, Stolina M, Dwyer D, Dougall WC, Hawkins N, Boyle WJ, Simonet WS, Sullivan JK (2009) Denosumab, a fully human monoclonal antibody to RANKL, inhibits bone resorption and increases BMD in knock-in mice that express chimeric (murine/human) RANKL. J Bone Miner Res 24:182–195

Lacey DL, Timms E, Tan HL, Kelley MJ, Dunstan CR, Burgess T, Elliott R, Colombero A, Elliott G, Scully S, Hsu H, Sullivan J, Hawkins N, Davy E, Capparelli C, Eli A, Qian YX, Kaufman S, Sarosi I, Shalhoub V, Senaldi G, Guo J, Delaney J, Boyle WJ (1998) Osteoprotegerin ligand is a cytokine that regulates osteoclast differentiation and activation. Cell 93:165–176

Li M, Shen Y, Qi H, Wronski TJ (1996) Comparison study of skeletal response to estrogen depletion at red and yellow marrow sites in rats. Anat Rec 245:472–480

Li X, Ominsky MS, Stolina M, Warmington KS, Geng Z, Niu QT, Asuncion FJ, Tan HL, Grisanti M, Dwyer D, Adamu S, Ke HZ, Simonet WS, Kostenuik PJ (2009a) Increased RANK ligand in bone marrow of orchiectomized rats and prevention of their bone loss by the RANK ligand inhibitor osteoprotegerin. Bone 45:669–676

Li X, Ominsky MS, Warmington KS, Morony S, Gong J, Cao J, Gao Y, Shalhoub V, Tipton B, Haldankar R, Chen Q, Winters A, Boone T, Geng Z, Niu QT, Ke HZ, Kostenuik PJ, Simonet WS, Lacey DL, Paszty C (2009b) Sclerostin antibody treatment increases bone formation, bone mass, and bone strength in a rat model of postmenopausal osteoporosis. J Bone Miner Res 24:578–588

Li Q, Ren G, Xu L, Wang Q, Qi J, Wang W, Zhou B, Han X, Sun C, Wu Q, Yu Y, Peng Z, Zheng S, Li D (2014) Therapeutic efficacy of three bispecific antibodies on collagen-induced arthritis mouse model. Int Immunopharmacol 21:119–127

Lill CA, Fluegel AK, Schneider E (2000) Sheep model for fracture treatment in osteoporotic bone: a pilot study about different induction regimens. J Orthop Trauma 14:559–566

Lill CA, Gerlach UV, Eckhardt C, Goldhahn J, Schneider E (2002) Bone changes due to glucocorticoid application in an ovariectomized animal model for fracture treatment in osteoporosis. Osteoporos Int 13:407–414

Ma YF, Ke HZ, Jee WSS (1994) Prostaglandin E2 adds bone to a cancellous bone site with a closed growth plate and low bone turnover in ovariectomized rats. Bone 15:137–146

MacLeay JM, Olson JD, Enns RM, Les CM, Toth CA, Wheeler DL, Turner AS (2004) Dietary-induced metabolic acidosis decreases bone mineral density in mature ovariectomized ewes. Calcif Tissue Int 75:431–437

Mbalaviele G, Dunstan CR, Sasaki A, Williams PJ, Mundy GR, Yoneda T (1996) E-cadherin expression in human breast cancer cells suppresses the development of osteolytic bone metastases in an experimental metastasis model. Cancer Res 56:4063–4070

Miller SC, Bowman BM, Miller MA, Bagi CM (1991) Calcium absorption and osseous organ-, tissue-, and envelope-specific changes following ovariectomy in rats. Bone 12:439–446

Miller RE, Roudier M, Jones J, Armstrong A, Canon J, Dougall WC (2008) RANK ligand inhibition plus docetaxel improves survival and reduces tumor burden in a murine model of prostate cancer bone metastasis. Mol Cancer Ther 7:2160–2169

Min H, Morony S, Sarosi I, Dunstan CR, Capparelli C, Scully S, Van G, Kaufman S, Kostenuik PJ, Lacey DL, Boyle WJ, Simonet WS (2000) Osteoprotegerin reverses osteoporosis by inhibiting endosteal osteoclasts and prevents vascular calcification by blocking a process resembling osteoclastogenesis. J Exp Med 192:463–474

Miyakoshi N, Sato K, Tsuchida T, Tamura Y, Kudo T (1999) Histomorphometric evaluation of the effects of ovariectomy on bone turnover in rat caudal vertebrae. Calcif Tissue Int 64:318–324

Mori R, Kodaka T, Soeta S, Sato J (2005) Preliminary study of histological comparison on the growth patterned of long-bone cortex in young calf, pig, and sheep. J Vet Med Sci 67: 1223–1229

Morony S, Capparelli C, Sarosi I, Lacey DL, Dunstan CR, Kostenuik PJ (2001) Osteoprotegerin inhibits osteolysis and decreases skeletal tumor burden in syngeneic and nude mouse models of experimental bone metastasis. Cancer Res 61:4432–4436

Mosekilde L, Sogaard CH, Danielson CC, Torring O, Nilsson MHL (1991) The anabolic effects of human parathyroid hormone (hPTH) on rat vertebral body mass are also reflected in the quality of bone, assessed by biomechanical testing: A comparison study between hPTH-(1–34) and hPTH- (1–84). Endocrinology 129:421–428

Mosekilde L, Danielsen DD, Knudsen UB (1993a) The effect of aging and ovariectomy on the vertebral bone mass and biomechanical properties of mature rats. Bone 14:1–6

Mosekilde L, Weisbrode SE, Safron JA, Stills HF, Jankowsky ML, Ebert DC, Danielsen CC, Sogaard CH, Franks F, Stevens ML, Paddock CL, Boyce RW (1993b) Evaluation of the skeletal effects of combined mild dietary calcium restriction and ovariectomy in Sinclair S-1 minipigs: a pilot study. J Bone Miner Res 8:1311–1321

Ochi H, Hara Y, Tagawa M, Shinomiya K, Asou Y (2010) The roles of TNFR1 in lipopolysaccharide-induced bone loss: dual effects of TNFR1 on bone metabolism via osteoclastogenesis and osteoblast survival. J Orthop Res 28:657–663

Oelzner P, Fleissner-Richter S, Bräuer R, Hein G, Wolf G, Neumann T (2010) Combination therapy with dexamethasone and osteoprotegerin protects against arthritis-induced bone alterations in antigen-induced arthritis of the rat. Inflamm Res 59:731–741

Ohshima S, Saeki Y, Mima T, Sasai M, Nishioka K, Nomura S, Kopf M, Katada Y, Tanaka T, Suemura M, Kishimoto T (1998) Interleukin 6 plays a key role in the development of antigen-induced arthritis. Proc Natl Acad Sci U S A 95:8222–8226

Ominsky MS, Li X, Asuncion FJ, Barrero M, Warmington KS, Dwyer D, Stolina M, Geng Z, Grisanti M, Tan HL, Corbin T, McCabe J, Simonet WS, Ke HZ, Kostenuik PJ (2008) RANKL inhibition with osteoprotegerin increases bone strength by improving cortical and trabecular bone architecture in ovariectomized rats. J Bone Miner Res 23:672–682

Ominsky MS, Vlasseros F, Jolette J, Smith SY, Stouch B, Doellgast G, Gong J, Gao Y, Cao J, Graham K, Tipton B, Cai J, Deshpande R, Zhou L, Hale MD, Lightwood DJ, Henry AJ, Popplewell AG, Moore AR, Robinson MK, Lacey DL, Simonet WS, Paszty C (2010) Two doses of sclerostin antibody in cynomolgus monkeys increases bone formation, bone mineral density, and bone strength. J Bone Miner Res 25:948–959

Park JS, Kwok SK, Lim MA, Kim EK, Ryu JG, Kim SM, Oh HJ, Ju JH, Park SH, Kim HY, Cho ML (2014) STA-21, a promising STAT-3 inhibitor that reciprocally regulates Th17 and Treg cells, inhibits osteoclastogenesis in mice and humans and alleviates autoimmune inflammation in an experimental model of rheumatoid arthritis. Arthritis Rheumatol 66:918–929

Pearce AI, Richards RG, Milz S, Schneider E, Pearce SG (2007) Animal models from implant biomaterial research in bone: a review. Eur Cell Mater 13:1–10

Peng Z, Tuukkanen J, Vaananen HK (1994) Exercise can provide protection against bone loss and prevent the decrease in mechanical strength of femoral neck in ovariectomized rats. J Bone Miner Res 9:1559–1564

Persson P, Gagnemo-Persson R, Hakanson R (1993) The effect of high or low dietary calcium on bone and calcium homeostasis in young male rats. Calcif Tissue Int 52:460–464

Pietschmann P, Skalicky M, Kneissel M, Rauner M, Hofbauer G, Stupphann D, Viidik A (2007) Bone structure and metabolism in a rodent model of male senile osteoporosis. Exp Gerontol 42:1099–1108

Pietschmann P, Rauner M, Sipos W (2008) Osteoporosis: an age-related and gender-specific disease – a mini-review. Gerontology 55:3–12

Pogoda P, Egermann M, Schnell JC, Priemel M, Schilling AF, Alini M, Schinke T, Rueger JM, Schneider E, Clarke I, Amling M (2006) Leptin inhibits bone formation not only in rodents but also in sheep. J Bone Miner Res 21:1591–1599

Redlich K, Hayer S, Maier A, Dunstan CR, Tohidast-Akrad M, Lang S, Türk B, Pietschmann P, Woloszczuk W, Haralambous S, Kollias G, Steiner G, Smolen JS, Schett G (2002) Tumor necrosis factor alpha-mediated joint destruction is inhibited by targeting osteoclasts with osteoprotegerin. Arthritis Rheum 46:785–792

Reinholz MM, Zinnen SP, Dueck AC, Dingli D, Reinholz GG, Jonart LA, Kitzmann KA, Bruzek AK, Negron V, Abdalla AK, Arendt BK, Croatt AJ, Sanchez-Perez L, Sebesta DP, Lönnberg H, Yoneda T, Nath KA, Jelinek DF, Russell SJ, Ingle JN, Spelsberg TC, Dixon HB, Karpeisky A, Lingle WL (2010) A promising approach for treatment of tumor-induced bone diseases: utilizing bisphosphonate derivatives of nucleoside antimetabolites. Bone 47:12–22

Ross AB, Bateman TA, Kostenuik PJ, Ferguson VL, Lacey DL, Dunstein CR, Simske SJ (2001) The effects of osteoprotegerin on the mechanical properties of rat bone. J Materials Sci 12:583–588

Sarkar S, Cooney LA, White P, Dunlop DB, Endres J, Jorns JM, Wasco MJ, Fox DA (2009) Regulation of pathogenic IL-17 responses in collagen-induced arthritis: roles of endogenous interferon-gamma and IL-4. Arthritis Res Ther 11:R158

Scholz-Ahrens KE, Delling G, Jungblut PW, Kallweit E, Barth CA (1996) Effect of ovariectomy on bone histology and plasma parameters of bone metabolism in nulliparous and multiparous sows. Z Ernahrungswiss 35:13–21

Scholz-Ahrens KE, Delling G, Stampa B, Helfenstein A, Hahne HJ, Açil Y, Timm W, Barkmann R, Hassenpflug J, Schrezenmeir J, Glüer CC (2007) Glucocorticosteroid-induced osteoporosis in adult primiparous Göttingen miniature pigs: effects on bone mineral and mineral metabolism. Am J Physiol Endocrinol Metab 293:E385–E395

Shahnazari M, Martin BR, Legette LL, Lachcik PJ, Welch J, Weaver CM (2009) Diet calcium level but not calcium supplement particle size affects bone density and mechanical properties in ovariectomized rats. J Nutr 139:1308–1314

Sigrist HM, Gerhardt C, Alini M, Schneider E, Egermann M (2007) The long-term effects of ovariectomy on bone metabolism in sheep. J Bone Miner Metab 25:28–35

Sipos W (1997) In-vitro Maturation und In-vitro Fertilisation canincer Oozyten unter besonderer Berücksichtigung der Supplementierung der In-vitro Maturationsmedien mit 17β-Östradiol und Progesteron. Thesis, University of Veterinary Medicine Vienna

Sipos W, Duvigneau JC, Hofbauer G, Schmoll F, Baravalle G, Exel B, Hartl R, Dobretsberger M, Pietschmann P (2005) Characterization of the cytokine pattern of porcine bone marrow-derived cells treated with $1\alpha,25(OH)_2D_3$. J Vet Med A 52:382–387

Sipos W, Kralicek E, Rauner M, Duvigneau JC, Worliczek HL, Schamall D, Hartl RT, Sommerfeld-Stur I, Dall'Ara E, Varga P, Resch H, Schwendenwein I, Zysset P, Pietschmann P (2011a) Bone and cellular immune system of multiparous sows are insensitive to ovariectomy and nutritive calcium shortage. Horm Metab Res 43:404–409

Sipos W, Zysset P, Kostenuik P, Mayrhofer E, Bogdan C, Rauner M, Stolina M, Dwyer D, Sommerfeld-Stur I, Pendl G, Resch H, Dall'Ara E, Varga P, Pietschmann P (2011b) OPG-Fc treatment in growing pigs leads to rapid reductions in bone resorption markers, serum calcium, and bone formation markers. Horm Metab Res 43:944–949

Sogaard CH, Danielsen CC, Thorling EB, Mosekilde L (1994) Long-term exercise of young and adult female rats: effect on femoral neck biomechanical competence and bone structure. J Bone Miner Res 9:409–416

Stolina M, Bolon B, Dwyer D, Middleton S, Duryea D, Kostenuik PJ, Feige U, Zack DJ (2008) The evolving systemic and local biomarker milieu at different stages of disease progression in rat collagen-induced arthritis. Biomarkers 13:692–712

Stolina M, Schett G, Dwyer D, Vonderfecht S, Middleton S, Duryea D, Pacheco E, Van G, Bolon B, Feige U, Zack D, Kostenuik P (2009a) RANKL inhibition by osteoprotegerin prevents bone loss without affecting local or systemic inflammation parameters in two rat arthritis models: comparison with anti-TNFalpha or anti-IL-1 therapies. Arthritis Res Ther 11:R187

Stolina M, Bolon B, Middleton S, Dwyer D, Brown H, Duryea D, Zhu L, Rohner A, Pretorius J, Kostenuik P, Feige U, Zack D (2009b) The evolving systemic and local biomarker milieu at

different stages of disease progression in rat adjuvant-induced arthritis. J Clin Immunol 29:158–174
Talbott SM, Rothkopf MM, Shapses SA (1998) Dietary restriction of energy and calcium alters bone turnover and density in younger and older female rats. J Nutr 128:640–645
Thomas ML, Ibarra MJ, Solcher B, Wetzel S, Simmons DJ (1988) The effect of low dietary calcium and calcium supplements on calcium metabolism and bone in the immature growing rat. Bone Miner 4:73–82
Turner AS (2002) The sheep as a model for osteoporosis in humans. Vet J 163:232–239
Turner RT, Vandersteenhoven JJ, Bell NH (1987) The effects of ovariectomy and 17 beta estradiol on cortical bone histomorphometry in growing rats. J Bone Miner Res 2:115–122
Turner AS, Park RD, Aberman HM, Villanueva AR, Nett TM, Trotter GW, Eckhoff DG (1993) Effects of age and ovariectomy on trabecular bone of the proximal femur and iliac crest in sheep. Trans Orthop Res Soc 18:548
Turner AS, Mallinckrodt CH, Alvis MR, Bryant HU (1995) Dose-response effects of estradiol implants on bone mineral density in ovariectomized ewes. Bone 17:421–427
Tyagi AM, Mansoori MN, Srivastava K, Khan MP, Kureel J, Dixit M, Shukla P, Trivedi R, Chattopadhyay N, Singh D (2014) Enhanced immunoprotective effects by anti-IL-17 antibody translates to improved skeletal parameters under estrogen deficiency compared with anti-RANKL and anti-TNF-α antibodies. J Bone Miner Res 29:1981–1992
Wang L, Banu J, McMahan CA, Kalu DN (2001) Male rodent model of age-related bone loss in men. Bone 29:141–148
Weinstein RS, Jilka RL, Parfitt AM, Manolagas SC (1998) Inhibition of osteoblastogenesis and promotion of apoptosis of osteoblasts and osteocytes by glucocorticoids. J Clin Invest 102:274–282
Westerlind KC, Wronski TJ, Ritman EL, Luo Z-P, An K-N, Bell NH, Turner RT (1997) Estrogen regulates the rate of bone turnover but bone balance in ovariectomized rats is modulated by prevailing mechanical strain. Proc Natl Acad Sci U S A 94:4199–4204
Wronski TJ, Yen CF (1992) The ovariectomized rat as an animal model for postmenopausal bone loss. Cells Mater (Suppl) 1:69–74
Wronski TJ, Walsh CC, Ignaszewski LA (1986) Histologic evidence for osteopenia and increased bone turnover in ovariectomized rats. Bone 7:119–124
Wronski TJ, Cintron M, Dann LM (1988) Temporal relationship between bone loss and increased bone turnover in ovariectomized rats. Calcif Tissue Int 42:179–183
Wronski TJ, Dann LM, Scott KS, Cintron M (1989) Long-term effects of ovariectomy and aging on the rat skeleton. Calcif Tissue Int 45:360–366
Wronski TJ, Dann LM, Horner SL (1990) Time course of vertebral osteopenia in ovariectomized rats. Calcif Tissue Int 46:101–110
Yoneda T, Michigami T, Yi B, Williams PJ, Niewolna M, Hiraga T (2000) Actions of bisphosphonate on bone metastasis in animal models of breast carcinoma. Cancer 88:2979–2988
Yoshitake K, Yokota K, Kasugai Y, Kagawa M, Sukamoto T, Nakamura T (1999) Effects of 16 weeks of treatment with tibolone on bone mass and bone mechanical and histomorphometric indices in mature ovariectomized rats with established osteopenia on a low-calcium diet. Bone 25:311–319
Yun TJ, Tallquist MD, Aicher A, Rafferty KL, Marshall AJ, Moon JJ, Ewings ME, Mohaupt M, Herring SW, Clarck EA (2001) Osteoprotegerin, a crucial regulator of bone metabolism, also regulates B cell development and function. J Immunol 166:1482–1491
Zheng Y, Zhou H, Brennan K, Blair JM, Modzelewski JRK, Seibel MJ, Dunstan CR (2007) Inhibition of bone resorption, rather than direct cytotoxicity, mediates the anti-tumour actions of ibandronate and osteoprotegerin in a murine model of breast cancer bone metastasis. Bone 40:471–478